

MULTI EPOCH SPATIALLY RESOLVED RADIO OBSERVATIONS OF BETELGEUSE’S WIND ACCELERATION REGION

EAMON O’GORMAN¹, GRAHAM M. HARPER¹, ALEXANDER BROWN², AND ANITA M. S. RICHARDS³

Draft version June 12, 2014

ABSTRACT

Previous VLA observations have only spatially resolved the stellar atmosphere at 0.7 cm but here we fully resolve the star at all wavelengths between 0.7 and 6.1 cm. New multi-epoch e-MERLIN data are urgently required.

Keywords: Radio continuum: stars — Stars: supergiants — Stars: individual (α Ori) — Stars: mass-loss — Stars: winds, outflows

1. INTRODUCTION

Red supergiants (RSGs) lose mass to the interstellar medium in the form of a massive ($\dot{M} \sim 10^{-7} - 10^{-4} M_{\odot} \text{ yr}^{-1}$) cool wind, with terminal velocities ($10 \lesssim v_{\infty} \lesssim 50 \text{ km s}^{-1}$) typically less than the photospheric escape velocity ($v_{\text{esc}} \sim 100 \text{ km s}^{-1}$). These winds are major contributors of heavy elements to the interstellar medium (ISM) and play a crucial role in stellar evolution (Chiosi & Maeder 1986), and also in explaining the frequency of supernovae in the galaxy (e.g., van Loon 2010). Despite their importance, the mechanisms responsible for the formation of these winds in late K and early M-type RSGs remain largely unknown. Dust is observed too far from the star to play a significant role in the mass-loss process (Danchi et al. 1994) and pulsation amplitudes are too low to initiate the mass-loss (Smith et al. 1989). Magnetohydrodynamic (MHD) waves (e.g., Thirumalai & Heyl 2012) and large convective cells (e.g., Josselin & Plez 2007) have been proposed as alternative potential mass-loss mechanisms in RSGs but spatially resolved multi-epoch observations of RSGs are required to test these competing theories.

1.1. Tracing Betelgeuse’s Mass Loss History

Betelgeuse (α Ori, M2Iab) is the closest isolated RSG ($d = 197 \pm 45 \text{ pc}$; Harper et al. 2008) and is therefore the prototype of the late K and early M spectral type RSG class. Its large angular diameter ($\phi_{\star} = 42.49 \pm 0.06 \text{ mas}$ in the K band, Ohnaka et al. 2011) coupled with its extended atmosphere makes it an excellent target for detailed multi-wavelength studies aiming to build a complete understanding of mass-loss in RSGs. Such studies have recently been carried out and have traced the ejected material over various spatial scales between the ISM and the photosphere. The wind-ISM interaction produces a multi-arc bow shock structure (Decin et al. 2012) and a detached H I shell elongated in the south-west direction (Le Bertre et al. 2012). Two distinct flows in its circumstellar envelope (CSE) were imaged at 1.3 mm by O’Gorman et al. (2012) which traced CO($J = 2 - 1$) on scales between $\sim 40 R_{\star}$ and $\sim 750 R_{\star}$.

These observations revealed an irregular CSE with a notable asymmetry in the south-west direction extending out to $\sim 200 R_{\star}$. Thermal infrared images using the Very Large Telescope (VLT) uncovered an envelope of inhomogeneous surface brightness up to $100 R_{\star}$, whose spectral energy distribution is typical of oxygen-rich dust (Kervella et al. 2011). These images also uncovered a ring-like structure at radius $20 - 45 R_{\star}$ which may be related to the dust condensation radius. The inner CSE was probed in the near-infrared with the VLT by Kervella et al. (2009) who discovered a molecular plume extending out to almost $6 R_{\star}$ in the south-west direction, which they attributed to the action of a photospheric giant convective cell. Indeed, the photospheric bright spots detected on Betelgeuse by Haubois et al. (2009) have now been attributed to presence of giant convective cells (Chiavassa et al. 2010). However, this does not provide definitive evidence that such convective cells are actually responsible for initiating the mass-loss.

1.2. Betelgeuse at Centimeter Wavelengths

Thermal free-free centimeter continuum emission directly probes the chromospheres and wind acceleration regions of RSGs; the regions identified as the most important for studies of mass-loss mechanisms in evolved stars (Holzer & MacGregor 1985). The first detailed study of Betelgeuse at centimeter wavelengths was carried out with the Very Large Array (VLA) by Newell & Hjellming (1982). The source was unresolved but the radio emission was interpreted as chromospheric in origin and extending from $1 - 4 R_{\star}$. This was in agreement with the Alfvén wave models to follow (Hartmann & Avrett 1984) and later Hubble Space Telescope (*HST*) spatially resolved ultraviolet observations (Gilliland & Dupree 1996; Uitenbroek et al. 1998). Spatially resolved VLA plus Multi-Element Radio Linked Interferometer Network (MERLIN) observations at 6 cm also confirmed the extended nature of the radio emitting region (Skinner et al. 1997).

Lim et al. (1998) used the VLA in its most extended (i.e., A) configuration to resolve Betelgeuse’s atmosphere at 0.7 cm and partially resolve it at 1.3, 2.0, 3.6, and 6 cm. Because the radio emission is thermal and optically thick, they were able to calculate the mean gas temperature as a function of radius, and found that the temperature decreased steadily from $\sim 3450 \text{ K}$ at $2 R_{\star}$, to $\sim 1370 \text{ K}$ at $7 R_{\star}$. They also detected an asymmetry in their 0.7 cm image which they attributed to the action of a large con-

¹ School of Physics, Trinity College Dublin, Dublin 2, Ireland

² Center for Astrophysics and Space Astronomy, University of Colorado, 389 UCB, Boulder, CO 80309, USA

³ Jodrell Bank Centre for Astrophysics, School of Physics and Astronomy, University of Manchester, Manchester M13 9PL, UK

vective cell. To reconcile their results with the extended ultraviolet emission, they concluded that the inner atmosphere must be inhomogeneous to accommodate the hot chromospheric plasma, but that the cooler gas must be 3 orders of magnitude more abundant. Harper & Brown (2006) used observations of the chromospheric tracer C II] $\lambda 2325 \text{ \AA}$ to confirm this low filling factor for the chromospheric gas.

lim, richards) (Teff=3600, ohnaka)

Why this paper, i.e. looking for evidence of emerlin e difference between the peak flux densities of these two "spots" is about 23 sigma

2. OBSERVATIONS AND DATA REDUCTION

The data were imaged within the Common Astronomical Software Application (CASA; ?) package. The xxx uvmodelfit was used while bounding the axis ratio between 0 and 1, and the position angle between 0 and 180.

Phase center was found using Reid & Menton

3. RESULTS

3.1. Visibilities

3.2. Radio Images

All are axially symmetric discuss fast switching (carilli paper)

3.3. Wind Thermal Profile

give formula

4. DISCUSSION

4.1. Radio Flux Density Variability

see Reid & Menton 1996 conf proceedings
see Drake conf proceedings
e-MERLIN flux is concentrated
see Harper_variability. ps
does flux go up as ang diam go up

4.2. Structure of Wind Acceleration Region

Thermal structure (Lim vs vs Ours vs e-MERLIN)
see Reid & Menton 1996 conf proceedings
Harper model

4.3. Where are the Hotspots?

No sign of hotspots (see Harpers pie town proceedings)
) See harper 2001 discussion emerlin rules out convective cells, magnetic fields?

5. CONCLUSIONS

The data presented in this paper were obtained with the Karl G. Jansky Very Large Array (VLA) which is an instrument of the National Radio Astronomy Observatory (NRAO). The NRAO is a facility of the National Science Foundation operated under cooperative agreement by Associated Universities, Inc. We wish to thank the NRAO helpdesk for their detailed responses to our CASA related queries. This publication has emanated from research conducted with the financial support of Science Foundation Ireland under Grant Number SFI11/RFP.1/AST/3064, and a grant from Trinity College Dublin.

Facilities: VLA.

REFERENCES

- Chiavassa, A., Haubois, X., Young, J. S., Plez, B., Josselin, E., Perrin, G., & Freytag, B. 2010, *A&A*, 515, A12
Chiosi, C., & Maeder, A. 1986, *ARA&A*, 24, 329
Danchi, W. C., Bester, M., Degiacomi, C. G., Greenhill, L. J., & Townes, C. H. 1994, *AJ*, 107, 1469
Decin, L., et al. 2012, *A&A*, 548, A113
Gilliland, R. L., & Dupree, A. K. 1996, *ApJ*, 463, L29
Harper, G. M., & Brown, A. 2006, *ApJ*, 646, 1179
Harper, G. M., Brown, A., & Guinan, E. F. 2008, *AJ*, 135, 1430
Hartmann, L., & Avrett, E. H. 1984, *ApJ*, 284, 238
Haubois, X., et al. 2009, *A&A*, 508, 923
Holzer, T. E., & MacGregor, K. B. 1985, in *Astrophysics and Space Science Library*, Vol. 117, Mass Loss from Red Giants, ed. M. Morris & B. Zuckerman, 229–255
Josselin, E., & Plez, B. 2007, *A&A*, 469, 671
Kervella, P., Perrin, G., Chiavassa, A., Ridgway, S. T., Cami, J., Haubois, X., & Verhoelst, T. 2011, *A&A*, 531, A117
Kervella, P., Verhoelst, T., Ridgway, S. T., Perrin, G., Lacour, S., Cami, J., & Haubois, X. 2009, *A&A*, 504, 115
Le Bertre, T., Matthews, L. D., Gérard, E., & Libert, Y. 2012, *MNRAS*, 422, 3433
Lim, J., Carilli, C. L., White, S. M., Beasley, A. J., & Marson, R. G. 1998, *Nature*, 392, 575
Newell, R. T., & Hjellming, R. M. 1982, *ApJ*, 263, L85
O’Gorman, E., Harper, G. M., Brown, J. M., Brown, A., Redfield, S., Richter, M. J., & Requena-Torres, M. A. 2012, *AJ*, 144, 36
Ohnaka, K., et al. 2011, *A&A*, 529, A163
Skinner, C. J., Dougherty, S. M., Meixner, M., Bode, M. F., Davis, R. J., Drake, S. A., Arens, J. F., & Jernigan, J. G. 1997, *MNRAS*, 288, 295
Smith, M. A., Patten, B. M., & Goldberg, L. 1989, *AJ*, 98, 2233
Thirumalai, A., & Heyl, J. S. 2012, *MNRAS*, 422, 1272
Uitenbroek, H., Dupree, A. K., & Gilliland, R. L. 1998, *AJ*, 116, 2501
van Loon, J. T. 2010, in *Astronomical Society of the Pacific Conference Series*, Vol. 425, Hot and Cool: Bridging Gaps in Massive Star Evolution, ed. C. Leitherer, P. D. Bennett, P. W. Morris, & J. T. Van Loon, 279

Table 1
Multi Epoch VLA A-Configuration Plus Pie Town Link Observations of Betelgeuse.

Date	Wavelength (cm)	Restoring Beam (mas \times mas)	Image rms (mJy/Beam)	θ_{maj} (mas)	$\theta_{\text{maj}}/\theta_{\text{min}}$	P.A. (deg)	F_{ν} (mJy)	T_b (K)
2004 Oct 21,30	0.7	39×26	0.37	99 ± 3	0.93 ± 0.04	92 ± 20	28.67 ± 0.53	2940 ± 170
	1.3	80×42	0.09	121 ± 2	13.88 ± 0.10	3140 ± 80
	2.0	121×91	0.08	158 ± 6	7.23 ± 0.15	2270 ± 130
	3.6	208×126	0.02	215 ± 7	0.87 ± 0.04	162 ± 7	3.34 ± 0.03	2110 ± 110
	6.1	377×264	0.02	315 ± 30	0.59 ± 0.13	173 ± 10	1.55 ± 0.04	1140 ± 160
	20.5	1262×889	0.03	≤ 889	0.25 ± 0.03	>260
2003 Aug 10,12	0.7	40×27	0.46	103 ± 4	0.89 ± 0.06	104 ± 16	28.05 ± 0.84	2760 ± 230
	1.3	80×42	0.17	122 ± 5	11.20 ± 0.24	2490 ± 150
	2.0	119×96	0.10	132 ± 10	0.87 ± 0.10	11 ± 27	5.88 ± 0.17	3040 ± 360
	3.6	204×139	0.03	193 ± 7	0.73 ± 0.06	152 ± 7	2.80 ± 0.04	2610 ± 170
	6.1	378×297	0.03	209 ± 49	1.22 ± 0.04	2040 ± 680
	20.5	1247×931	0.04	≤ 931	0.26 ± 0.03	>250
2002 Apr 12,13	1.3	91×59	0.18	134 ± 9	0.76 ± 0.07	36 ± 10	8.96 ± 0.24	2170 ± 250
	2.0	131×98	0.39	166 ± 16	0.63 ± 0.10	41 ± 11	5.32 ± 0.23	2420 ± 450
	3.6	224×155	0.03	234 ± 9	0.73 ± 0.05	40 ± 7	2.66 ± 0.04	1690 ± 110
	20.5	1398×1146	0.06	≤ 1146	0.38 ± 0.06	>240
2002 Feb 17,18	1.3	83×48	0.14	120 ± 4	0.91 ± 0.04	30 ± 13	10.87 ± 0.17	2750 ± 140
	2.0	128×90	0.11	140 ± 13	5.38 ± 0.22	2150 ± 300
	3.6	200×135	0.03	199 ± 8	2.85 ± 0.04	1830 ± 110
	20.5	1312×951	0.05	≤ 951	0.30 ± 0.05	>270
2001 Jan 02	1.3	78×42	0.08	124 ± 2	0.92 ± 0.02	40 ± 8	12.58 ± 0.08	2920 ± 70
2000 Dec 23	0.7	44×20	0.18	98 ± 2	0.92 ± 0.02	0 ± 7	29.02 ± 0.30	3070 ± 100

Notes.- The restoring beam and image rms noise values were obtained using uniform weighting and include the Pie Town antenna baselines. The position angles (measured in degrees east of north) of the restoring beams in these images are not given here but are all between 30° and 70° . The major axis of the stellar radio disk, θ_{maj} , the axis ratio of the major and minor radio disks, $\theta_{\text{maj}}/\theta_{\text{min}}$, the position angle, P.A., and the total flux density, F_{ν} , are all derived from the best-fit uniform-brightness (T_b) elliptical-disk models.

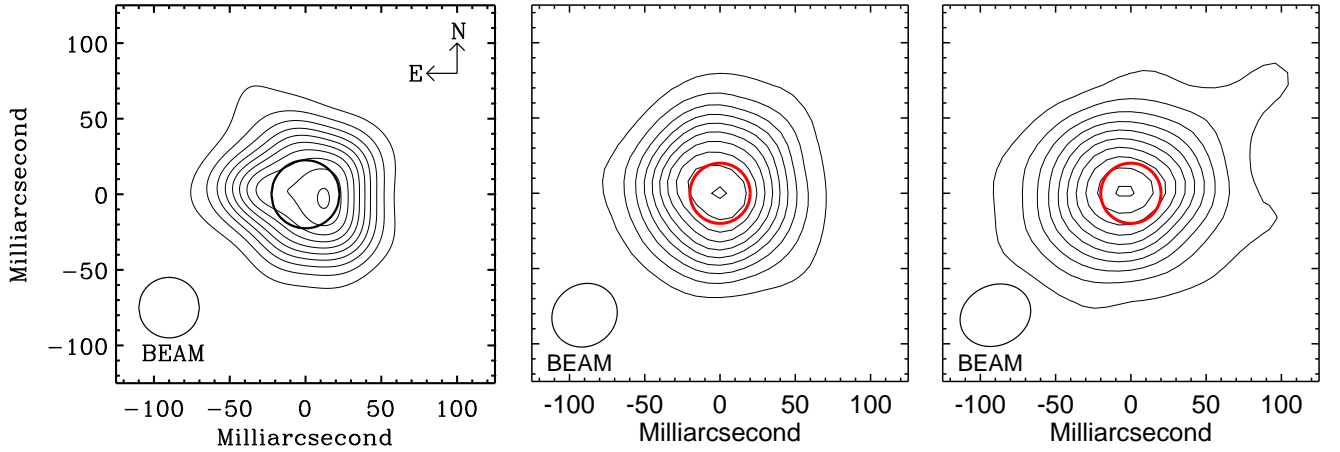


Figure 1. VLA A-configuration maps of Betelgeuse at 0.7 cm.